Nanostructure formation in InAs/InP(001) heteroepitaxy: Importance of surface reconstruction

T. J. Krzyzewski and T. S. Jones*
Department of Chemistry, University of Warwick, Coventry CV4 7AL, United Kingdom
(Received 17 March 2008; published 7 October 2008)

Scanning tunneling microscopy has been used to study the deposition by molecular-beam epitaxy of thin InAs films on InP(001) substrates and compared with InAs growth on GaAs(001) under nominally identical conditions. In contrast to InAs/GaAs, InAs growth on InP does not proceed via a Stranski-Krastanov type mechanism, with a well-defined two-dimensional–three-dimensional growth mode transition, but instead a gradual and continuous surface roughening process occurs even from the earliest stages of deposition. Average height and surface roughness measurements indicate the absence of lateral surface correlations generated between adjacent elongated wires formed at higher deposition coverages. The origin of this growth behavior is attributed to the pregrowth formation of a self-templating arsenic-stabilized InP(001)-(2×4) surface, which is prepatterned on the atomic scale for the growth of highly anisotropic nanostructures.

DOI: 10.1103/PhysRevB.78.155307 PACS number(s): 68.37.−d, 68.55.−a, 68.65.−k

I. INTRODUCTION

The concerted research efforts aimed at controling the properties of III–V semiconductor nanostructures formed during self-organized growth in lattice-mismatched heteroepitaxy have led, among other successes, to the fabrication of InAs/GaAs-based quantum dot (QD) devices which operate at the technologically important wavelength of 1.3 μm. However, extending this to longer wavelengths remains challenging in this highly mismatched (~7%) system.[1] Use of the InAs/InP growth system, which has a smaller lattice mismatch (~3.2%) and in principle offers a more attractive route for producing nanostructures for longer-wavelength applications, has been hampered by its significantly greater complexity compared to InAs/GaAs, in particular due to the formation and undesirable coexistence of more than one type of nanostructure on (001) surfaces, including quantum wires (QWRs), quantum dashes (QDashs), and QDs.[2] Identifying appropriate pathways for the selective growth of single-type nanostructure arrays in the InAs/InP(001) system is therefore an essential step in their development and fabrication for use in device applications.

To further our understanding of InAs/InP nanostructure formation, we have used rapid-quench scanning tunneling microscopy (STM) to study as a function of nominal InAs coverage (θ) the growth by molecular-beam epitaxy (MBE) of thin InAs films on InP(001) substrates and compared these with InAs grown on GaAs(001) under nominally identical experimental conditions. Our results show that a true 2D $\rightarrow$3D (where 2D and 3D stand for two-dimensional and three-dimensional, respectively) Stranski-Krastanov (SK) growth mode transition does not occur during direct deposition of InAs on InP(001). Instead, elongated wires form as a result of a gradual and continuous surface roughening process where lateral growth is significantly inhibited in the [110] but not in the [−110] or the vertical [001] direction even at the earliest stages of deposition. The average height ($\langle h\rangle$) and root-mean-square roughness ($\langle w\rangle$) of the surface both increase linearly as a function of θ for all coverages studied, consistent with the absence of surface correlations between adjacent wires along [110] and the evolution of an uncorrelated growth front. The origin of this behavior is attributed to the predeposition formation of a self-templating As-stabilized InP surface which is in effect prepatterned on an atomic scale for highly anisotropic growth. Its existence can be traced back to the unique way in which the surface strain inevitably built up after P-As exchange during the predeposition exposure of an InP surface to an As flux is relaxed within the confines of a (2×4)-reconstructed surface structure. A simple atomic-scale model for the mechanism of strain relaxation and the resulting enhancement of the inherent (2×4) growth anisotropy is also proposed.

II. EXPERIMENTAL DETAILS

The experiments were carried out in a combined STM-MBE system equipped with reflection high-energy electron diffraction (RHEED). Epi-ready n+ doped singular InP(001) ($\pm0.1°$) substrates were outgassed under a residual As_2 flux ($<1\times10^{-8}$ mbar) at ~300 °C for up to 1 h. Prior to removal of the native oxide, the As_2 flux was increased to 1×10^{-6} mbar; this was maintained throughout the cleaning, annealing, and deposition stages of all experiments. The substrate temperature was then rapidly ramped up to ~520–540 °C and the sample annealed for 75–150 s. Once the weak (1×1) RHEED pattern typical of an oxidized surface changed to a strong one indicating the presence of a (4×2) surface reconstruction, the temperature was immediately reduced to 350–370 °C. The $(1\times1)\rightarrow(4\times2)$ phase change is direct with no intermediate transitional structure detectable by RHEED. This is indicative of the formation of an As-stabilized InP(001) surface[3] since a high-temperature (4×2) phase is energetically unfavorable[4] and does not exist on pure InP(001) surfaces under normal MBE conditions. On cooling, a further reconstruction change to a (2×4) surface occurs at ~460 °C, again consistent with the phase changes observed on As-stabilized InAs(001) surfaces. RHEED and STM both confirmed that the (4×2) and the (2×4) surfaces are atomically flat. After the sample temperature was stabilized at 350–370 °C, it was slowly raised to a growth temperature of 400–450 °C and up to 3.4 nm of InAs ($\theta\sim10$

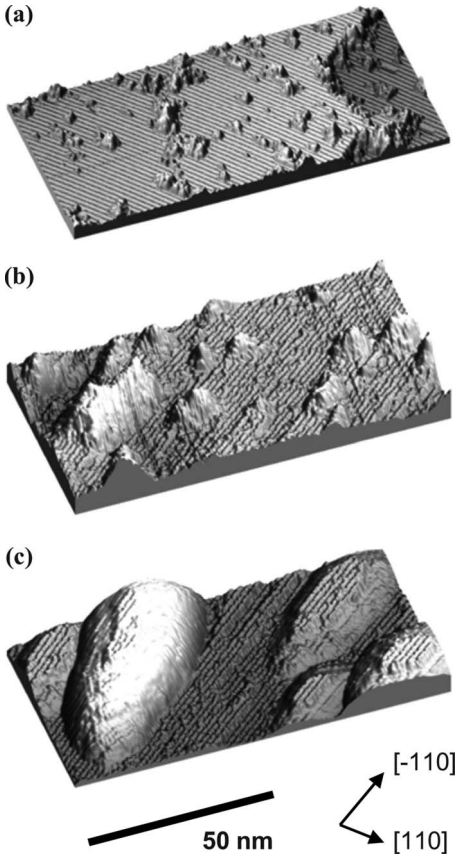

FIG. 1. 3D projections of filled states STM images (100×50 nm^2) of oxidized InP(001) surfaces after exposure to As_2 for: (a) ~60 min at 480 °C, followed by ~20 min at 500 °C [sample was quenched at 500 °C and exhibits a (4×2) reconstruction but not the (2×4) structure observed at lower temperatures]; (b) ~60 min at 520 °C, followed by 5 min at 540 °C [irreversible surface degradation via formation of In droplets up to 2.5 nm in height]; and (c) ~2 min anneal at 560 °C [flat top QD-like structures up to 3.5 nm in height].

ML) was deposited at a growth rate of ~0.045 ML s^{-1} (V:III ratio ~12:1). Immediately after deposition, the sample was quenched [initial cooling rate ~50 °C s^{-1} (Ref. 5)] into the adjacent room temperature STM chamber, where samples were scanned with a bias voltage of −2.5–3.0 V and a current of 0.2–0.3 nA. Comparative InAs deposition ($\theta \leq 2.7$ ML) was also carried out on GaAs(001) substrates at 400 °C under the same nominal experimental conditions.

Careful control over the preparation of the InP(001) surface prior to InAs deposition was found to be very important to ensure subsequent high-quality nanostructure formation. The STM images in Fig. 1, which are 3D projections of filled states images (100×50 nm^2), highlight some of the different morphologies obtained when using different surface preparation methods. Thermal oxide desorption under high As_2 fluxes ($>2.5 \times 10^{-6}$ mbar) and low substrate temperatures (<500 °C) was also found to produce high-quality surfaces [Fig. 1(a)] but requires much longer exposure times. Exposure at high temperatures (>540 °C) or long annealing times (>180 s) invariably resulted in significant degradation of the surface [Fig. 1(b)] or the formation of a 3D surface morphology [Fig. 1(c)]. The surface structure in both Figs. 1(b) and 1(c) is a typical (2×4) reconstruction, unlike that observed on similarly degraded surfaces obtained after heating oxidized InP(001) substrates in ultrahigh vacuum without the presence of a group V flux.[6] This shows that the presence of the As flux is essential in stabilizing the surface directly after thermal oxide removal. The existence of a top As-stabilizing layer was confirmed by reducing the temperature of the InP(001) substrate thermally cleaned under an As flux to below 350 °C. The RHEED pattern changed from a (2×4) to a weak (2×3) reconstruction; this is indicative of the presence of an InAs top layer since $(n \times 3)$ reconstructions are commonly observed on InAs(001) substrates but not on InP(001).[7]

III. RESULTS AND DISCUSSION

Filled states STM topographs (100×100 nm^2) of the surface taken before and after deposition of InAs on As-stabilized InP(001) at 400 °C are shown in Figs. 2(a)–2(d), together with the corresponding height cross sections. The As-stabilized InP(001) starting surface exhibits a (2×4) reconstruction [Fig. 2(a)] and is atomically flat with $\langle w \rangle \sim 0.12$ nm and $\langle h \rangle \sim 0.42$ nm. These values are comparable to those measured on other (001) III–V semiconductor surfaces prepared by more commonly used methods such as thermal oxide desorption followed by buffer layer growth[8] and indicate that thermal desorption of the native oxide from InP(001) under an As flux is a very effective method of obtaining a high-quality surface without the need for a P supply provided that only short annealing times are used to minimize the degree of As/P exchange.[9] It should be pointed out that since the As/P exchange is very rapid and takes place within at most a few seconds even at low temperatures,[3] the predeposition surface stabilization step which normally takes place under an arsenic flux prior to any epitaxial growth will invariably lead to the formation of a thin InAs film on top of the InP substrate. This can be 1–5 ML thick[10,11] and means that InAs growth does not occur on a P-terminated InP substrate, as is often considered to be the case, but on a pre-existing *strained* InAs layer. Consequently, the surface shown in Fig. 2(a) resembles the actual starting surface for InAs deposition much more closely than any native InP reconstruction.

Deposition of InAs onto the As-stabilized starting surface does not lead to alloying and pseudomorphic 2D growth as observed for the coherent stages of InAs/GaAs(001) epitaxy[12] but instead results in the formation of an atomically roughened surface where the grown layers are *incomplete*. This can be seen most clearly in Fig. 2(b), which corresponds to $\theta = 1.35$ ML InAs deposition. Pits more than 1 ML deep can already be observed on the surface (circled in the STM image and highlighted by arrows on the corresponding cross section). Further InAs deposition leads to increased roughening of the surface. The anisotropy of the surface morphology perpendicular to the growth direction also increases, with noticeable elongation in the [−110] direction. Layer growth remains incomplete, and filling in of the pits observable at the lower coverage does not occur [e.g., Fig.

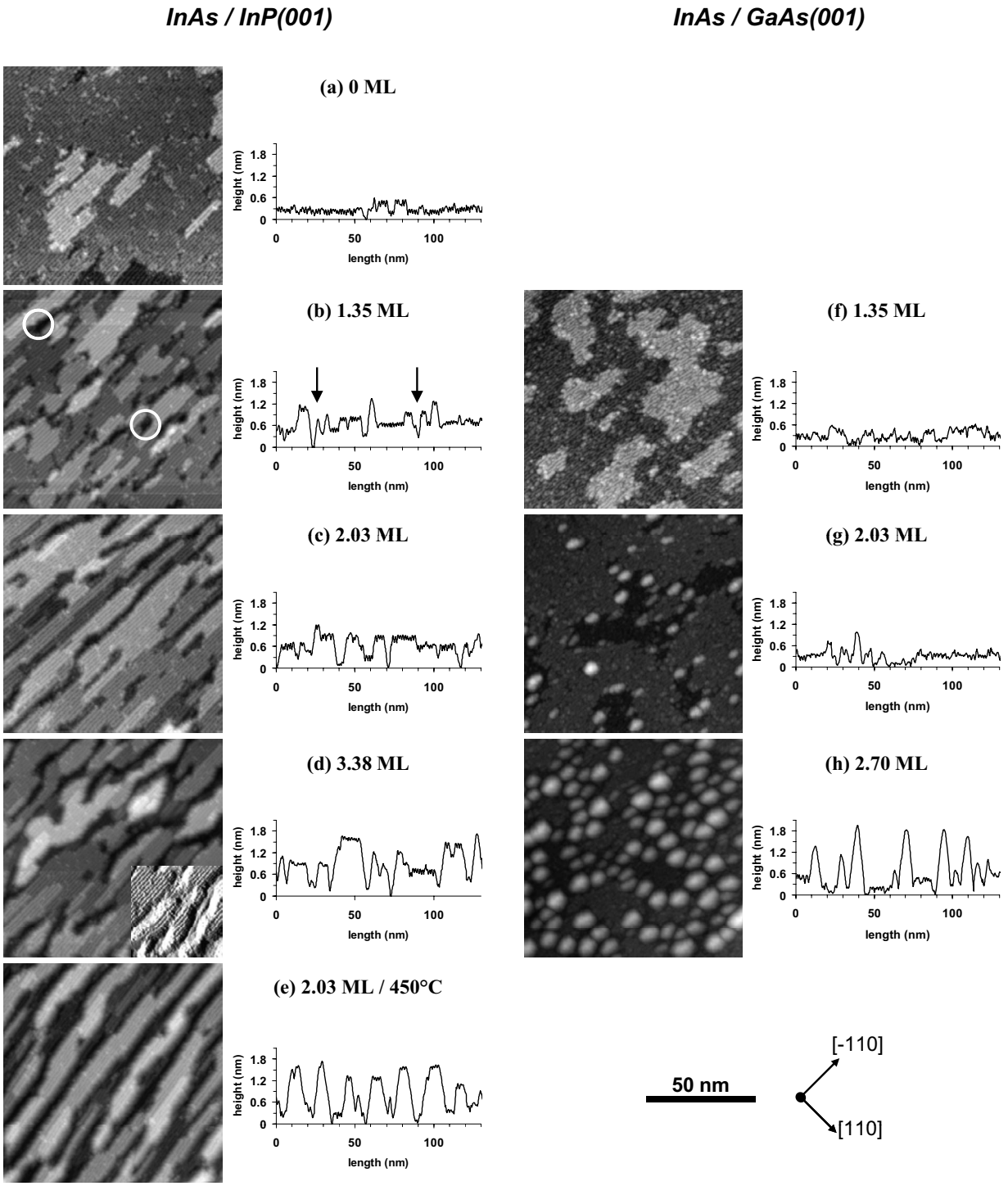

FIG. 2. Filled states STM topographs (100×100 nm^2) of surface morphology (a) before and after InAs deposition on [(b)–(d)] InP(001) at 400 °C and (e) InP(001) at 450 °C and [(f)–(h)] GaAs(001) at 400 °C. Part of image (d) has been differentiated to highlight the surface reconstruction. All corresponding cross sections taken diagonally from top left to bottom right corner through the entire image.

2(c) corresponding to θ=2.03 ML]. At higher coverages, poorly defined highly elongated QWR-like structures with a height of up to 1.8 nm (~6 ML) become apparent; see, e.g., Fig. 2(d) for θ=3.38 ML. Their lateral and vertical size increase gradually as a function of θ, with no sudden onset of 3D islanding. Even at this very high nominal coverage, no reconstruction changes or evidence for alloying can be observed. The dimer rows of the (2×4) reconstruction remain clearly visible on the top layer of the surface [see inset of Fig. 2(d)]. The evolution of the surface morphology for deposition at 450 °C is qualitatively very similar to that observed at 400 °C, except that the surface roughening is much more rapid at the higher temperature. However, it is still continuous and gradual, and no alloying, changes in reconstruction, or any sudden growth mode transition is observed. An STM topograph of the surface after deposition of 2.03

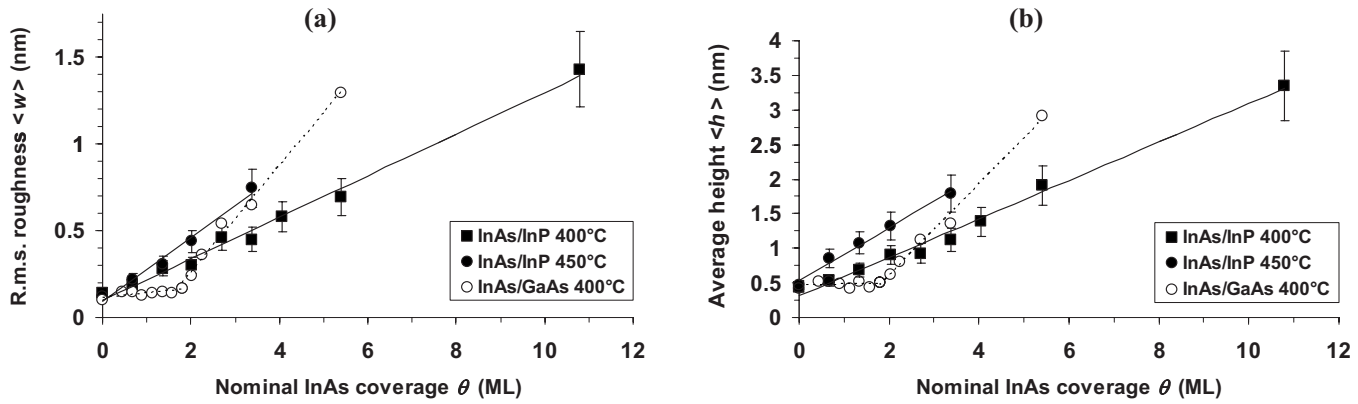

FIG. 3. (a) rms surface roughness $\langle w \rangle$ and (b) average height $\langle h \rangle$ measured directly from several STM topographs as a function of amount of InAs deposited for InAs deposition on InP(001) at 450 °C (filled circles), InP(001) at 400 °C (filled squares), and GaAs(001) at 400 °C (empty circles). Linear fits for InAs/InP growth at 400 and 450 °C are also shown.

ML InAs at 450 °C is shown in Fig. 2(e). While the heights and to a lesser extent the lengths of the wires are much larger compared to those observed at the same nominal coverage at 400 °C [cf. Figs. 2(c) and 2(e)], the widths remain almost unchanged, with typical values in the range 15–20 nm.

The evolution of surface morphology as observed by STM for InAs growth on GaAs(001) at 400 °C [Figs. 2(f)–2(h)] is qualitatively similar to that reported previously for higher temperatures.[13] InAs deposition on the atomically smooth $c(4\times4)$ reconstructed GaAs(001) starting surface initially results in the formation of a complete alloyed 2D wetting layer (WL) with an $a(1\times3)$ reconstruction [Fig. 2(f)], with further deposition eventually leading to a 2D $\rightarrow$3D growth mode transition at a critical coverage (θ_{crit}) of $\sim$1.8 ML, and the nucleation of small QDs [Fig. 2(g)]. At higher coverages, the surface morphology is dominated by a high density of well-defined QDs, slightly elongated along [−110] [Fig. 2(h)].

The surface features observed during InAs deposition on InP(001) are not distinct and are difficult to define particularly at low θ. Figure 3(a) shows the variation in $\langle w \rangle$, measured directly from several STM topographs, as a function of nominal coverage for deposition on InP(001) at both 400 and 450 °C, and for direct comparison, InAs deposition on GaAs(001) at 400 °C. The roughness increases continuously and linearly as a function of InAs deposition on InP(001) at both temperatures, with the rate of increase larger at the higher temperature. By contrast, InAs/GaAs(001) growth is characterized by an initial pseudomorphic 2D layer-by-layer growth phase where $\langle w \rangle$ remains constant, followed by a sudden growth mode transition at θ_{crit}, after which $\langle w \rangle$ increases rapidly but also linearly with θ. The variation in $\langle h \rangle$ as a function of θ for both InAs/GaAs(001) and InAs/InP(001) growth is shown in Fig. 3(b) and is qualitatively very similar to that observed for $\langle w \rangle$.

For InAs/GaAs, strain-driven alloying enables at least partial strain relaxation and 2D growth up to θ_{crit}; all new material deposited beyond θ_{crit} is incorporated into new or existing QDs. Since strain effects are only important at very earliest stages of QD formation[14] and factors such as In desorption or mass transport from the WL do not contribute at this low growth temperature,[15] it is reasonable to expect that $\langle w \rangle$ will vary linearly with time (and therefore θ as the deposition rate is constant). For InAs/InP growth at higher temperatures, enhanced As/P exchange during the stabilization step before growth is likely to be responsible for the more rapid surface roughening at 450 °C than at 400 °C; the effective thickness of the InAs layer formed increases as a function of temperature. This is likely since P desorption is a thermally activated process and does not depend on the presence of As atoms.[16] However, although *in situ* RHEED patterns are indicative of a 2D surface morphology and STM topographs of the surface prior to growth at the higher temperature do not indicate any significant 3D surface roughening, some degree of alloying cannot be ruled out.[17,18]

Our results indicate that in contrast to InAs/GaAs(001), an SK-type mechanism does not operate during InAs/InP(001) heteroepitaxy, at least for the range of experimental conditions studied. This difference can be attributed to the effect of group V element exchange before InAs deposition, as it is the key factor which greatly influences InAs growth on InP(001), but is not present when the substrate is GaAs(001). Unfortunately the amount of InAs generated during the rapid group V exchange during the pregrowth exposure of the InP(001) to an As flux is difficult to measure directly and needs to be inferred from other data; it also varies with temperature.[19] In consequence, not only will the *actual* InAs surface coverage be invariably greater than the *nominal* coverage, i.e., the amount of InAs supplied to the surface, but most importantly, the thickness of the pregrowth InAs layer may easily exceed θ_{crit} for that temperature (particularly at high temperatures and/or high As fluxes), leading to a 2D$\rightarrow$3D growth mode transition and formation of 3D nanostructures without any direct InAs deposition having taken place[20,21] [see, e.g., Fig. 1(c)]. The nature of the 2D $\rightarrow$3D growth mode transition is also different during direct InAs deposition on InP compared to GaAs: in contrast to the sharp transition observed under a wide range of experimental conditions during direct InAs deposition on GaAs(001), the onset of 3D InAs growth on InP(001) substrates is not abrupt even under far-from-equilibrium conditions[22] or may occur only *after* the In supply has been terminated during post-growth annealing under an As flux.[23,24] Furthermore, since the 2D$\rightarrow$3D growth mode transition is considered a strain

relief mechanism during heteroepitaxial growth, the onset of 3D growth is normally expected to coincide with stress relaxation and the appearance of a spotty RHEED pattern, indicative of the formation of 3D surface features; chevrons may also form although their appearance and angle depends on the shape of the 3D islands produced.[25] While a clear reduction in the rate of stress increase is coincident with the appearance a spotty RHEED pattern and chevrons for direct InAs deposition on GaAs(001),[26] this is not the case for InAs growth on InP(001).[27] Here, some strain relaxation precedes the appearance of 3D features in RHEED, suggesting that a strain relief mechanism other than a growth mode transition may be operating. In addition, other InAs/InP growth studies[28] have shown that chevrons appear at the same time as a spotty RHEED pattern at nominal coverages as low as 0.8 ML and the chevron angle only increases gradually from 0° to >20° over a wide nominal coverage range (>1 ML). This is in contrast to changes in the RHEED pattern observed during InAs growth on GaAs, where chevrons appear rapidly within less than 0.1 ML of θ_{crit} with angles of 10° and above; changes in the chevron angle are also not as large as those observed on InP(001) surfaces.[29] These subtle but important differences point to the contrasting ways in which heteroepitaxial strain is accommodated within the two growth systems and highlight gaps in our detailed understanding of InAs growth on InP compared to the more extensively researched and relatively well-understood InAs/GaAs system, in particular the relative effects of strain and reconstruction. The gradual and continuous evolution of the InAs/InP surface morphology as shown in Fig. 2 suggests that unlike for InAs growth on GaAs where strain effects dominate reconstruction effects at all but the lowest coverages, the role of the initial reconstruction is far more crucial in the InAs/InP system.

For InAs growth on InP, the strain perpendicular to the growth direction (parallel to the surface) is in fact about an order of magnitude *lower* than the strain in the growth direction (perpendicular to the surface).[30] This is a consequence of significant bond lengthening parallel to the growth direction in an attempt to accommodate some of the lattice mismatch between the film and the substrate. While this could be regarded as the main driving force behind the *general* roughening of the interface and may explain the linear relationship between $\langle w \rangle$ and time, it is the movement of atoms *in* (and not normal to) the plane of the surface that is important in determining the detailed evolution of the surface morphology, in particular the type of nanostructure formed. The absence of any reconstruction change and the lack of clear evidence for alloying during InAs deposition on InP(001) suggests that it is the microscopic structure of the As-stabilized (2×4)-reconstructed InP surface which plays the crucial role in determining the detailed evolution of surface morphology during growth in this material system. Although this influence has been highlighted in a number of studies,[28,31,32] it is not yet fully understood at the atomic scale. Since As/P exchange—which takes place prior to any InAs deposition—effectively "locks in" the (2×4) surface structure, it blocks any kinetic pathway to a lower energy, possibly alloyed reconstruction,[33] and any misfit strain after As/P exchange must be accommodated only within the (2×4) structure itself; this cannot occur isotropically parallel to the surface due to its inherent asymmetry. González *et al.*[34] proposed that the resulting anisotropic strain relaxation along the two orthogonal $\langle 110 \rangle$ directions of the (2×4) surface is responsible for the formation of highly elongated nanostructures during InAs/InP(001) growth.

A schematic of the InP surface before and after deposition of the first 2 ML of InAs, with proposed strain relaxation pathways is shown in Fig. 4. To accommodate the larger As atoms and longer In-As bonds once exchange has taken place, it is possible for dimer pairs in the uppermost surface layer to bend away from each other slightly across the dimer rows in the [110] direction [see arrows in Fig. 4(b)]. This is not possible along the dimer rows in the orthogonal [−110] direction, or for any dimers in the trenches, with bond elongation only in the [001] direction instead {tetragonal distortion normal to the surface [Fig. 4(a)]}. The InAs surface prior to deposition is therefore fully strained along [−110] [Fig. 4(c)] but partially relaxed in the [110] direction [Fig. 4(d)], resulting in surface diffusion anisotropy and ultimately the formation of nanostructures which are laterally asymmetric, as proposed by González *et al.*[34]

While this simple model can account qualitatively for the elongation of InAs/InP(001) nanostructures, it does not provide sufficient explanation for quantitative aspects of their growth, in particular the extreme anisotropies of these structures, which often have length/width ratios exceeding 50/1. It is also not clear from the model why there is a preference for the formation of continuous QWRs instead of, for example, an array of elongated QDs aligned along [−110], as observed for InGaAs growth on GaAs(001) with a mismatch very close to that of InAs/InP (Ref. 35) or why a similar dependence of the type of nanostructure formed on the anisotropy of the reconstruction is not found for InAs growth on GaAs(001). Here, preferential QD or QWR formation would be expected on, respectively, a symmetric $c(4\times4)$ or an asymmetric (2×4) starting surface, but instead QDs form irrespective of the starting reconstruction.[36] Furthermore, theoretical studies have found that the adatom diffusivity on inorganic semiconductor surfaces generally *decreases* at compressive strains;[37,38] indeed, this has often been attributed to the existence of surface reconstructions. In a simple anisotropic strain relaxation model, such an effect would in fact inhibit diffusion along the less relaxed (i.e., more strained) [−110] direction compared to [110] and might therefore erroneously suggest QWR elongation in [110] direction. Other studies which only take into account the influence of strain anisotropy on diffusion but ignore surface morphology effects[39] can also correctly predict the formation of elongated 3D nanostructures for InAs/InP (elastic anisotropy strength $\boldsymbol{A} \sim 2$ for both InAs and InP) but again incorrectly predict their alignment, in this case in the [100] direction instead of the experimentally observed [−110] direction.

A proposed extension of the anisotropic strain relaxation model showing subtle but crucial changes in the local atomic-level structure of the (2×4) surface is shown in Figs. 4(e)–4(h). The outward flexing of the dimer pairs along [110] makes the bottom of the trenches less favorable aggregation sites for any freshly deposited material compared to the top of existing dimer rows since locally the effective lattice con-

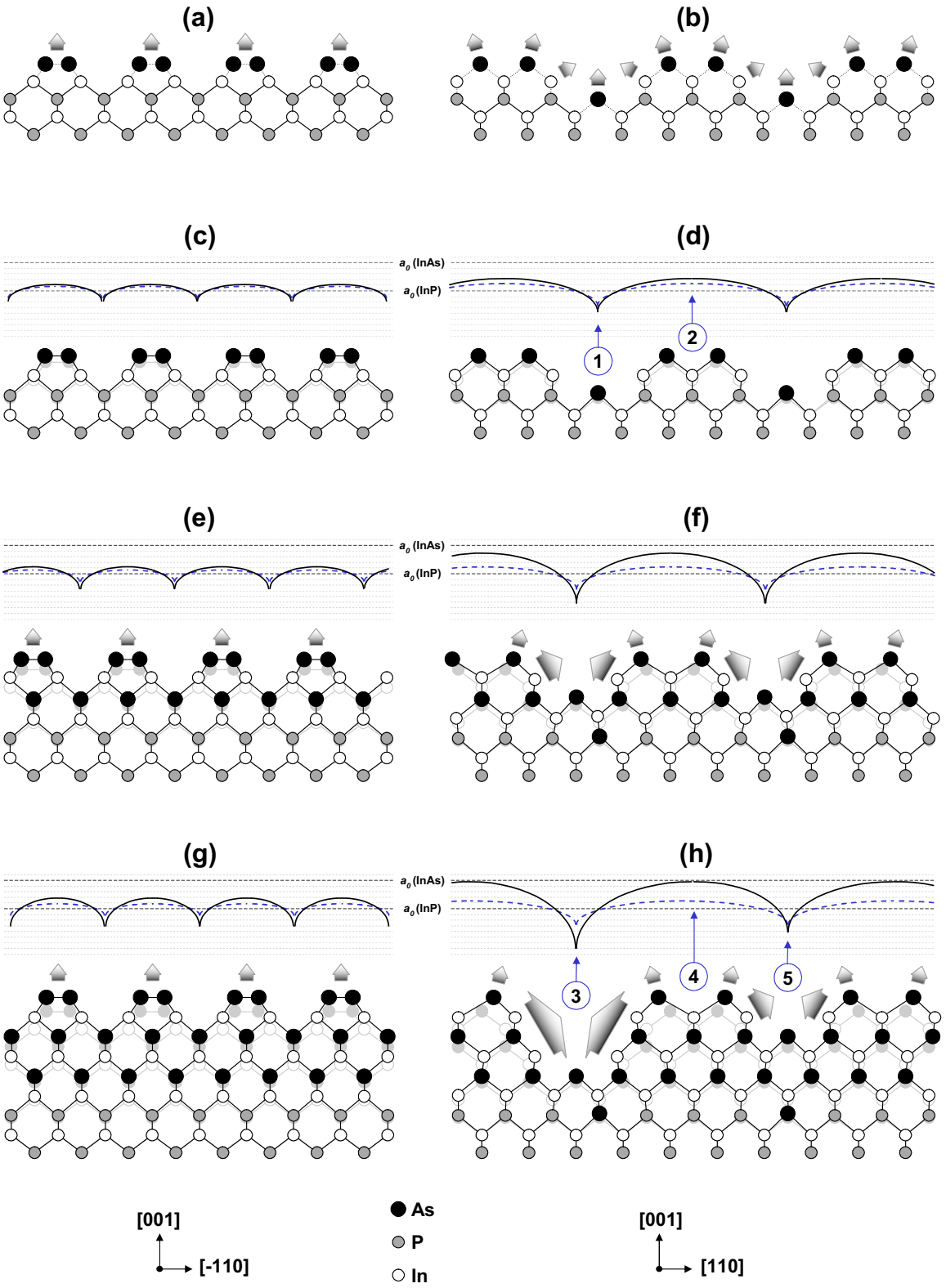

FIG. 4. (Color online) Schematic of proposed strain relaxation mechanism on an ideal (2×4)-reconstructed InP(001) surface [(a)–(d)] before and [(e)–(h)] after growth of InAs. Cross sections perpendicular (left-hand side) and parallel (right-hand side) to the dimer row direction of an InP-(2×4) surface after: (a)–(b) As/P exchange with no strain relaxation, (c)–(d) As/P exchange with partial strain relaxation, (e)–(f) deposition of first InAs ML, and (g)–(h) deposition of second InAs ML. Shaded gray arrows indicate direction of movement of atoms relative to their positions in an ideal unstrained InP-(2×4) structure (shown in light gray). Different types of In aggregation sites have been numbered 1–5. The variation in the in-plane local lattice constant relative to the bulk InP $[a_0(\mathrm{InP})]$ and InAs $[a_0(\mathrm{InAs})]$ lattice constants along each direction is also shown above the corresponding cross sections for an unstrained (dashed line) and strained (solid line) surface.

stant within the trench [Fig. 4(d), site 1] is smaller (i.e., less InAs like) than on the uppermost surface layers [Fig. 4(d), site 2]. This difference is larger than for an unstrained (2×4) surface. No strongly preferred aggregation sites are created along [−110] as atom movement and bond distortion is only possible in the [001] direction and not parallel to [−110] [Fig. 4(e)]. As the number of InAs layers increases, the relative ease with which the uppermost dimer pairs can flex out along [110] increases [shown with shaded gray arrows in Figs. 4(f) and 4(h)]. The relative differences in the local strain field at different sites increase and the probability of material aggregating in a deep trench [where the lattice constant is least InAs like; Fig. 4(h), site 3] compared to aggregation on top of the uppermost dimers [where the local lattice constant is most InAs-like; Fig. 4(h), site 4] or in a shallower trench [Fig. 4(h), site 5)] decreases further. This effect is cumulative and its strength is enhanced as θ increases. Trenches more than 1 ML deep can be observed already at InAs coverages below 2 ML ["pits" in Fig. 2(b)], and they act as areas of zero growth during InAs deposition, inhibiting In diffusion and lateral growth along [110]. In the orthogonal [−110] direction, atom movement and bond distortion are only possible in the [001] direction and not parallel to [−110]; the way the local lattice constant varies depends very weakly (if at all) on the number of InAs MLs deposited [e.g., compare Figs. 4(e) and 4(g)]. No preferential aggregation sites are created, and growth along [−110] remains uninhibited. Since the ease of diffusion across the pits will decrease with increasing pit depth, the rate of lateral expansion of the QWRs in the [110] direction will quickly tend to zero, with growth remaining uninhibited only laterally in the [−110] direction. This can easily account for the extreme elongation of the QWRs in one direction only, as diffusion in the orthogonal surface direction is simply too limited under normal growth conditions. It is worthy to note that even though the lengths of 3D nanostructures formed during InAs growth on InP under a wide range of experimental conditions can vary over three orders of magnitude from the nanometer to the micrometer range, their widths remain remarkably constant and consistently fall in the 10–30 nm range irrespective of whether the nanostructures formed are QWRs (Refs. 2 and 40) or QDs.[41] This may be viewed as further evidence for the proposed existence of a large diffusion barrier in the [110] direction only. Since the height of the diffusion barrier is large but finite, it might be expected that highly "nonequilibrium" growth conditions, for example, a very high growth rate or temperature, lead to the formation of nanostructures other than QWRs; this does indeed occur with QD formation observed for MBE growth of InAs on singular nonpatterned InP(001) substrates at growth rates of up to 1.8 ML s^{-1}.[22]

With the InAs/InP QWRs effectively growing independently of each other, the growth behavior in the system can be compared in principle to that expected on a highly misoriented or a narrow stripe patterned substrate. This can be described by simple growth models, and it is not surprising that InAs/InP(001) growth appears to be consistent with a very simple random deposition growth mechanism,[42] where $\langle w\rangle$ and $\langle h\rangle$ vary linearly with time and hence θ if the deposition rate is constant. This behavior is typical of an *uncorrelated* surface and, in this case, is clearly a consequence of the inability to build up surface correlations in the [110] direction across the QWRs. Although it is extremely unlikely that such a simple mechanism actually operates during MBE growth under the experimental conditions studied, it captures the essential characteristics of the growth process, namely, the lack of lateral surface correlations, which are a direct consequence of the existence and significant strain-induced enhancement of morphological and energetic asymmetries in this system. The evolution of the growth front during InAs deposition is thus predetermined by the characteristics of the starting surface prior to growth. This is in stark contrast to InAs growth on GaAs(001), where the pregrowth surface structure and morphology is much less important, and does not significantly affect the type or properties of the nanostructures formed during the latter stages of growth.

It must be emphasized that the type of strain relaxation pathway proposed in Fig. 4 is possible irrespective of the exact chemical composition of the surface, in particular whether the dimers in the top layers are pure As-As or mixed In-As;[33] it is the *local* trench-row structure of the (2×4) reconstruction maintained throughout the growth process which is the key factor in the formation of highly asymmetric surface structures. Furthermore, our discussion only applies to InAs grown directly on As-stabilized InP and does not cover any deposition of InAs on InGaAs buffer layers grown on InP; in these cases QDs are formed much more readily than QWRs (Ref. 43) and InP is simply treated as a convenient substrate for the growth of an unstrained InGaAs alloy.

It is also important to point out that if differences in experimental methodology and analysis techniques are taken into account, our work is fully consistent with other studies of the initial stages of InAs growth on InP where the formation of QWRs was interpreted in terms of an SK-type mechanism,[27,28] with a 2D→3D growth mode transition followed by 3D nanostructure growth, instead of the gradual and continuous surface roughening seen here. One key difference is that previous studies were carried out at much higher temperatures and As fluxes, and it is conceivable that a conventional SK-type mechanism may play a more prominent role under these experimental conditions. However, it is also probable that QWR formation mechanisms other than SK were not considered because not only was the low InAs coverage regime (<1.5 ML) not investigated in detail in these studies but also the effects of the postgrowth annealing were not taken into account. The analysis techniques used also impose fundamental limits on what can be observed, which means that subtle but very important changes in surface morphology, especially during the 2D phase of InAs growth on InP, might not be observed clearly. For example, a surface which is roughening due to strain but lacks distinct isolated 3D features will not induce clear observable changes in the corresponding RHEED patterns, e.g., compare the surfaces shown in Figs. 2(a) and 2(b), which both exhibit indistinguishable (2×4) RHEED patterns.

IV. CONCLUSIONS

We have used rapid-quench MBE-STM to study the growth of thin InAs films on InP(001) as a function of cov-

erage. The surface morphology was found to roughen continuously and gradually from the earliest stages of deposition and no evidence was found for a well-defined 2D-3D growth mode transition as observed in the corresponding studies of InAs growth on GaAs(001). The linear variation in the average height and surface roughness as a function of coverage reflects the absence of lateral correlations in the [110] direction between adjacent QWRs formed at higher coverages. This can be attributed to the pregrowth formation of an As-stabilized (2×4)-reconstructed InP surface, which was effectively prepatterned on an atomic scale for highly anisotropic growth. A possible model for the formation of this self-templating surface and its influence on subsequent growth is also proposed.

ACKNOWLEDGMENTS

The authors were grateful for financial support from the Engineering and Physical Sciences Research Council (EPSRC), U.K.

*FAX:+44 (0)24-7652-4112; t.s.jones@warwick.ac.uk

[1] V. M. Ustinov and A. E. Zhukov, Semicond. Sci. Technol. **15**, R41 (2000).
[2] O. Bierwagen and W. T. Masselink, Appl. Phys. Lett. **86**, 113110 (2005).
[3] C. H. Li, L. Li, D. C. Law, S. B. Visbeck, and R. F. Hicks, Phys. Rev. B **65**, 205322 (2002).
[4] W. G. Schmidt and F. Bechstedt, Surf. Sci. **409**, 474 (1998).
[5] T. J. Krzyzewski and T. S. Jones, J. Appl. Phys. **96**, 668 (2004).
[6] C. D. MacPherson, R. A. Wolkow, C. E. J. Mitchell, and A. B. McLean, Phys. Rev. Lett. **77**, 691 (1996).
[7] B. Junno, S. Jeppesen, M. S. Miller, and L. Samuelson, J. Cryst. Growth **164**, 66 (1996).
[8] A. Khatiri, J. M. Ripalda, T. J. Krzyzewski, G. R. Bell, C. F. McConville, and T. S. Jones, Surf. Sci. **548**, L1 (2004).
[9] D. C. Law, Y. Sun, C. H. Li, S. B. Visbeck, G. Chen, and R. F. Hicks, Phys. Rev. B **66**, 045314 (2002).
[10] G. Hollinger, D. Gallet, M. Gendry, C. Santinelli, and P. Viktorovitch, J. Vac. Sci. Technol. B **8**, 832 (1990).
[11] A. Tabata, T. Benyattou, G. Guillot, M. Gendry, G. Hollinger, and P. Viktorovitch, J. Vac. Sci. Technol. B **12**, 2299 (1994).
[12] J. G. Belk, C. F. McConville, J. L. Sudijono, T. S. Jones, and B. A. Joyce, Surf. Sci. **387**, 213 (1997).
[13] T. J. Krzyzewski, P. B. Joyce, G. R. Bell, and T. S. Jones, Surf. Sci. **517**, 8 (2002).
[14] T. J. Krzyzewski, P. B. Joyce, G. R. Bell, and T. S. Jones, Phys. Rev. B **66**, 201302(R) (2002).
[15] P. B. Joyce, T. J. Krzyzewski, G. R. Bell, B. A. Joyce, and T. S. Jones, Phys. Rev. B **58**, R15981 (1998).
[16] M. U. González, J. M. Garcia, L. González, J. P. Silveira, Y. González, J. D. Gómez, and F. Briones, Appl. Surf. Sci. **188**, 188 (2002).
[17] M. Taskinen, M. Sopanen, H. Lipsanen, J. Tulkki, T. Tuomi, and J. Ahopelto, Surf. Sci. **376**, 60 (1997).
[18] N. Carlsson, T. Junno, L. Montelius, M.-E. Pistol, L. Samuelson, and W. Seifert, J. Cryst. Growth **191**, 347 (1998).
[19] S. Yoon, Y. Moon, T.-W. Lee, E. Yoona, and Y. D. Kim, Appl. Phys. Lett. **74**, 2029 (1999).
[20] T. Kawamura, K. Akahane, Y. Okada, and M. Kawabe, Jpn. J. Appl. Phys., Part 2 **38**, L720 (1999).
[21] H. Yang, P. Ballet, and G. J. Salamo, J. Appl. Phys. **89**, 7871 (2001).
[22] B. Bansal, M. R. Gokhale, A. Bhattacharya, and B. M. Arora, J. Appl. Phys. **101**, 094303 (2007).
[23] H. Marchand, P. Desjardins, S. Guillon, J.-E. Paultre, Z. Bougrioua, R. Y.-F. Yip, and R. A. Masut, Appl. Phys. Lett. **71**, 527 (1997).
[24] L. González, J. M. García, R. García, F. Briones, J. Martínez-Pastor, and C. Ballesteros, Appl. Phys. Lett. **76**, 1104 (2000).
[25] T. Hanada, B.-H. Koo, H. Totsuka, and T. Yao, Phys. Rev. B **64**, 165307 (2001).
[26] J. M. Garcia, J. P. Silveira, and F. Briones, Appl. Phys. Lett. **77**, 409 (2000).
[27] D. Fuster, B. Alén, L. González, Y. González, J. Martínez-Pastor, M.-U. González, and J. M. García, Nanotechnology **18**, 035604 (2007).
[28] H. R. Gutierrez, M. A. Cotta, and M. M. G. de Carvalho, Appl. Phys. Lett. **79**, 3854 (2001).
[29] T. Kudo, T. Inoue, T. Kita, and O. Wada, *19th International Conference on Indium Phosphide and Related Materials, Matsue, Japan, May 14–18, 2007*, Conference Proceedings – Indium Phosphide and Related Materials (IEEE, 2007), p. 303–306.
[30] M. D. Robertson, J. C. Bennett, A. M. Webb, J. M. Corbett, S. Raymond, and P. J. Poole, Ultramicroscopy **103**, 205 (2005).
[31] E. Dupuy, P. Regreny, Y. Robach, M. Gendry, N. Chauvin, E. Tranvouez, G. Bremond, C. Bru-Chevallier, and G. Patriarche, Appl. Phys. Lett. **89**, 123112 (2006).
[32] D. Fuster, M. U. González, Y. González, and L. González, Surf. Sci. **600**, 23 (2006).
[33] W. G. Schmidt, Appl. Phys. A: Mater. Sci. Process. **75**, 89 (2002).
[34] M. U. González, L. González, J. M. Garcia, Y. González, J. P. Silveira, and F. Briones, Microelectron. J. **35**, 13 (2004).
[35] M. Schmidbauer, Z. M. Wang, Y. I. Mazur, P. M. Lytvyn, G. J. Salamo, D. Grigoriev, P. Schäfer, R. Köhler, and M. Hanke, Appl. Phys. Lett. **91**, 093110 (2007).
[36] T. J. Krzyzewski, P. B. Joyce, G. R. Bell, and T. S. Jones, Surf. Sci. **482-485**, 891 (2001).
[37] E. Penev, P. Kratzer, and M. Scheffler, Phys. Rev. B **64**, 085401 (2001).
[38] A. van de Walle, M. Asta, and P. W. Voorhees, Phys. Rev. B **67**, 041308(R) (2003).
[39] P. Liu, Y. W. Zhang, and C. Lu, Phys. Rev. B **67**, 165414 (2003).
[40] H. Parry, M. J. Ashwin, and T. S. Jones, J. Appl. Phys. **100**, 114305 (2006).
[41] G. Saint-Girons, A. Michon, I. Sagnes, G. Beaudoin, and G. Patriarche, Surf. Sci. **601**, 2765 (2007).
[42] A.-L. Barabasi and H. E. Stanley, *Fractal Concepts in Surface Growth* (Cambridge University Press, Cambridge, England, 1995), Chap. 4.
[43] Z. H. Zhang, G. W. Pickrell, K. L. Chang, H. C. Lin, K. C. Hsieh, and K. Y. Chen, Appl. Phys. Lett. **82**, 4555 (2003).